Fabrication and characterization of sliced multilayer transmission grating for X-ray region

Qiushi Huang (黄秋实)[1], Haochuan Li (李浩川)[1], Jingtao Zhu (朱京涛)[1*], Xiaoqiang Wang (王晓强)[1], Zhanshan Wang (王占山)[1], Lingyan Chen (陈玲燕)[1], and Yongjian Tang (唐永建)[2]

[1]*Key Laboratory of Advanced Micro-Structured Materials, MOE, Institute of Precision Optical Engineering, Department of Physics, Tongji University, Shanghai 200092, China*

[2]*Research Center of Laser Fusion, China Academy of Engineering Physics, Mianyang 621900, China*

[*]*Corresponding author: jtzhu@tongji.edu.cn*

Received February 15, 2012; accepted March 14, 2012; posted online May 16, 2012

To develop high quality dispersion optics in the X-ray region, the sliced multilayer transmission grating is examined. Dynamical diffraction theory is used to calculate the diffraction property of this volume grating. A WSi_2/Si multilayer with a d-spacing of 14.3 nm and bi-layer number of 300 is deposited on a super-polished silicon substrate by direct current magnetron sputtering technology. To make the transmission grating, the multilayer is sliced and thinned in the cross-section direction to a depth of 23–25 μm. The diffraction efficiency of the grating is measured at $E = 8.05$ keV, and the 1st-order efficiency is 19%. The sliced multilayer grating with large aspect ratio and nanometer period can be used for high efficiency and high dispersion optics in the X-ray region.

OCIS codes: 050.1950, 310.1860, 340.7480.
doi: 10.3788/COL201210.090501.

With the development of various deposition technologies, multilayers with thousands of layers can now be produced while still maintaining the thickness deviation of each layer within 0.1 nm[1,2]. These smart multilayers have been widely used in astronomical physics, synchrotron radiation, plasma diagnosis, and so on. Apart from the reflection optics realized by high reflectivity multilayer mirrors[3], another critical element in the extreme ultraviolet (EUV) and X-ray region is the dispersion optics. Conventional dispersion optics is usually provided with gratings[4−6] that are fabricated by etching methods. However, transmission gratings used in the hard X-ray region have to fulfill a very large aspect ratio (i.e., the depth of the grating groove divided by the line-width) in order to achieve a practical diffraction efficiency due to the dynamical effect[7,8]. Moreover, new optics in the X-ray region require higher dispersion power that, in turn, needs much larger groove density, i.e., very small period of the structure. These harsh requirements cannot be satisfied by etching techniques; as an alternative, sliced multilayer grating is a good solution for these problems. The slicing and thinning process can produce a multilayer grating with much larger aspect-ratio that can greatly increase the diffraction efficiency of hard X-ray[9]. By depositing a thick multilayer with a layer thickness of only several nanometers, the dispersion power of gratings can be increased[10]. In this letter, a WSi_2/Si multilayer of 300×14.3-nm periods is deposited and then sliced and polished to create a transmission grating. The diffraction efficiency of the grating is measured at 8.05 keV. The measured results demonstrate that the sliced multilayer transmission grating is very promising for applications in high efficiency and high dispersion optics in the X-ray region.

In the X-ray region, the transmission grating is required to have a smaller period (in nanometer) and larger depth, i.e., higher aspect ratio. The kinematical diffraction theory is no more suitable for these volume gratings. Instead, the dynamical diffraction theory has to be applied and must consider the interaction and coupling effect between the incident and diffraction waves of different orders inside the grating[7,11]. Thus, the diffraction efficiency is related to the depth of grating and the fulfillment of the Bragg condition. Only when the length of the interaction area is correctly chosen and the Bragg condition of a certain order, $2D\sin\theta = l\lambda$, is satisfied can the diffraction efficiency be enhanced[12]. A schematic of the sliced multilayer transmission grating is shown in Fig. 1. To calculate the theoretical efficiency of the grating, the one-dimensional coupled wave theory (1D-CWT) is used[11,13,14]. The multilayer grating is made up of two materials A (high-z) and B (low-z) alternatively with arbitrary thickness ratio, $\gamma = d_{\rm A}/(d_{\rm A}+d_{\rm B})$, where $d_{\rm A}$ and $d_{\rm B}$ are the layer thicknesses for materials A and B, respectively. Thus, the grating is described by a Fourier expansion of the periodically changing permittivity given by

$$\varepsilon(\vec{r}) = \bar{\varepsilon} + \Delta\varepsilon \cdot 2\gamma \cdot \mathrm{i} \cdot \sum_{h=1}^{\infty} \mathrm{sinc}(h\pi\cdot\gamma)\cdot\sin(h\vec{G}\cdot\vec{r}), \quad (1)$$

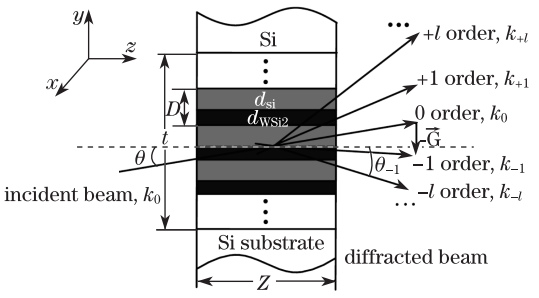

Fig. 1. Schematic illustration of the transmission sliced multilayer grating.

where, $\bar{\varepsilon} = \varepsilon_{\rm B} + (\varepsilon_{\rm A} - \varepsilon_{\rm B}) \cdot \gamma$ is the average permittivity, $\Delta\varepsilon$ is the difference of permittivities between two materials, and $\vec{G}$ is the grating vector. Assuming the grating is illuminated by a plane wave with wave vector of $\vec{k}_0$, the wave field inside the grating can be written as a sum of different orders of waves:

$$\overrightarrow{E(r)} = E_0 \sum_{l=-\infty}^{\infty} A_l(\vec{r}) \exp(-\mathrm{i}\vec{\rho}_l \cdot \vec{r}), \tag{2}$$

where E_0 is the field amplitude $E(z = 0)$, l is the diffraction order, $A_l(\vec{r})$ is the complex wave amplitude, and $\vec{\rho}_l$ is the wave vector of different diffraction orders, $\vec{\rho}_l = \vec{\rho}_0 + l\vec{G}$.

By inserting $\varepsilon(\vec{r})$ and $E(\vec{r})$ into the wave equation

$$\nabla^2 \overrightarrow{E(r)} - \vec{k}_0^2 \varepsilon(\vec{r}) \overrightarrow{E(r)} = 0, \tag{3}$$

a series of coupled differential equations of amplitudes $A_l(\vec{r})$ is obtained. Neglecting the 2nd-order derivatives, the 1st-order differential equations can be solved by a numerical method that finally yields the diffraction efficiency of different orders, $\eta_l = A_l(z)A_l^*(z)$. The detailed solving process can be found in Refs. [11,13,14]. According to this method, the diffraction efficiency of a multilayer grating with a period of $D = 14.3$ nm and a thickness ratio of $\gamma = 0.47$ is calculated at $E = 8.05$ keV. Both the ideal case (i.e., the incident angle satisfying the Bragg condition, $\theta = \theta_{\rm B} = 0.31°$ for the 1st order) and the non-tilted case (i.e., incident angle, θ=0°) are calculated, and the results are shown in Fig. 2.

The diffraction efficiency in the ideal case is oscillated with the depth which reaches a maximum of 62% at a depth of $z = 7.3$ μm. The second enhancement of the efficiency is achieved at a depth of around 24 μm, whereas the efficiency is 25% due to the larger absorption. In the non-tilted case, the efficiency is close to zero, because it is significantly deviated from the Bragg condition.

The designed multilayer grating consisted of a bi-layer number of 300 (corresponding to grating grooves number, N) with a total thickness of 4.3 μm. Deposition of this microns-thick multilayer causes tremendous accumulated stress, which can result in the buckling or peeling of layers during the following sampling process. Meanwhile, the presence of sharp interfaces of the multilayer is an important condition in achieving ideal grating performance. Thus, the material combination of the sliced

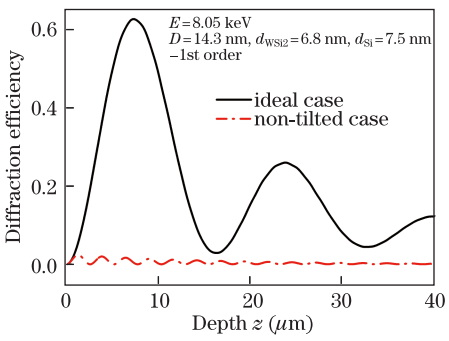

Fig. 2. Diffraction efficiency of the 1st-order sliced multilayer transmission grating versus grating depth.

multilayer grating must solve both of these problems. The WSi_2/Si multilayer has been demonstrated to be very suitable for the deposition of a thick multilayer due to its stable stress property[15,16]; it has also shown sharp interfaces with a small roughness[17]. In this study, the material combination of WSi_2/Si was selected to fabricate the multilayer grating. The sliced multilayer transmission grating was fabricated in two steps: the multilayer deposition and the sampling process. Firstly, a WSi_2/Si multilayer with a d-spacing of 14.3 nm and bi-layer number of 300 was deposited on a super-polished silicon substrate by direct current (DC) magnetron sputtering technology[18]. The working gas was Ar, and the working pressure was set at 0.2 Pa. It took 14 h to deposit this 4.3-μm-thick multilayer. The multilayer structure was characterized using grazing incident X-ray reflectance (GIXR) measurement. The measured d-spacing of the multilayer was $D = 14.3$ nm, and the layer thicknesses of WSi_2 and Si were $d_{\rm WSi2} = 6.8$ nm and $d_{\rm Si} = 7.5$ nm, respectively.

After deposition, the multilayer sample was sliced perpendicular to the surface. In order to protect the multilayer, another Si substrate was glued onto the surface to make a sandwich structure. Then, both cross-sections of the sandwich sample were grinded and polished to a thin depth, z, corresponding to the peak position shown in Fig. 2. The detailed sampling process has been illustrated elsewhere[19]. The depth of the multilayer grating was measured by a stylus profiler. Due to the difficulty of thinning the depth to below 10 μm, the fabricated depth in this letter reached a range of 23–25 μm, with an aspect ratio larger than 3 000. The surface roughness (RMS) of the cross-section, measured by atomic force microscopy (AFM) was ~0.5 nm. The cross-section of the multilayer grating was observed by a scanning electron microscope (SEM), as shown in Fig. 3. All the interfaces were sharp and flat, while the multilayer structure was preserved after slicing, repeated grinding, and polishing.

To study the diffraction efficiency of the sliced multilayer transmission grating, the sample was measured using a high resolution X-ray diffractometer and the X-ray source was Cu Kα_1 line ($E = 8.05$ keV). The diffraction geometry used in the measurement was the same as that shown in Fig. 1. The y-axis is defined as the layer growth direction of multilayer grating, whereas the z-axis is the depth direction of grating, i.e., perpendicular to the surface of the cross-section. The x-axis is the length direction of the multilayer grating. The divergence angle of the incident X-ray beam in the y-axis direction is 0.007°. In order to measure the diffraction efficiency quantitatively, a slit with a width of 40 μm was inserted into the incident beam path just in front of the multilayer grating. For the ideal case, both the grating equation, $D(\sin\theta + \sin\theta_l) = l\lambda$, and the Bragg condition, $2D\sin\theta = l\lambda$, are satisfied, making θ equal to θ_l. Thus, the grating was first measured in the ideal case by scanning in the specular direction (Q_z scan)[20]. Diffraction efficiency in the non-tilted case is measured by setting the incident angle, θ at 0° and performing the detector scan. The measured results are shown in Fig. 4. Sharp diffraction peaks of ±3 orders are clearly observed in the ideal case, thus indicating a well-ordered structure. According to the positions of the Bragg peaks

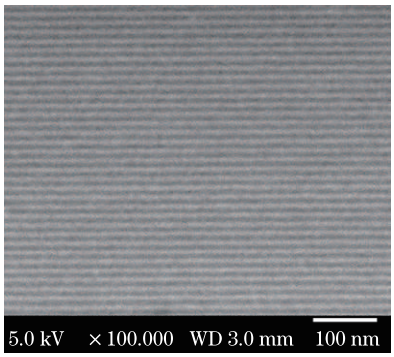

Fig. 3. SEM image of the multilayer structure after the sampling process.

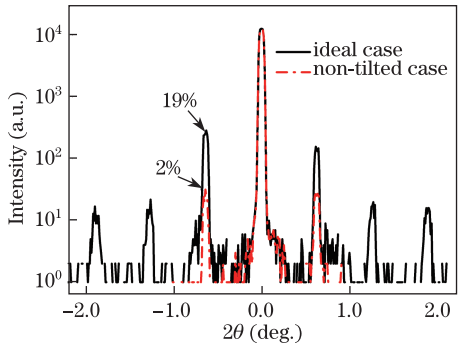

Fig. 4. Diffraction efficiency measurements of the multilayer grating in the ideal and non-tilted cases.

in different orders, the period of multilayer grating is D = 14.1 nm[20], which is almost the same with the as-deposited value. The absolute efficiency is obtained by normalizing the intensity of Bragg peaks with the incident intensity. In the ideal case, the highest diffraction efficiency of ±1 orders are achieved at the incident angle of $\theta = \theta_B = 0.31°$, which is the same as the design. The measured 1st-order efficiency is 19%, while the theoretical value shown in Fig. 2 is 25%. The asymmetric intensity of the +1 and −1 orders could be caused by small damages of the multilayer structure induced in the sampling process. The efficiency in the non-tilted case is much lower, only about 2%. The measured results are mainly consistent with the theoretical calculation, which proves that the sliced multilayer transmission grating with large aspect-ratio can achieve high diffraction efficiency in hard X-ray region.

In conclusion, the sliced multilayer transmission grating is developed in this letter. A WSi_2/Si multilayer with a d-spacing of 14.3 nm and bi-layer number of 300 is deposited on a super-polished silicon substrate by DC magnetron sputtering technology. Then, the multilayer is sliced into pieces and its cross-section is thinned and polished to a depth ranging from 23 to 25 μm to create the transmission grating. The diffraction efficiency of the grating is measured using an X-ray diffractometer at Cu Kα_1 line (E = 8.05 keV), and the 1st-order efficiency is as high as 19%. The sliced multilayer grating with large aspect-ratio and nanometer period is successfully fabricated. It can be used as high dispersion optics in the X-ray region. More efforts can be made in future studies to improve the performance of this sliced multilayer grating.

This work was supported by the National Natural Science Foundation of China (Nos. 10825521 and 10905042), the National "973" Program of China (No. 2011CB922203), and the Natural Science Foundation of Shanghai (No. 09ZR1434300).

References

1. Y. Platonov, V. Martynov, A. Kazimirov, and B. Lai, Proc. SPIE **5537,** 161 (2004).
2. C. Liu, R. Conley, A. T. Macrander, J. Maser, H. C. Kang, M. A. Zurbuchen, and G. B. Stephenson, J. Appl. Phys. **98,** 113519 (2005).
3. E. Spiller, Appl. Opt. **15,** 2333 (1976).
4. V. V. Martynov and Yu. Platonov, Rev. Sci. Instrum. **73,** 1551 (2002).
5. M. L. Schattenburg, R. J. Aucoin, R. C. Fleming, I. Plotnik, J. Porter, and H. I. Smith, Proc. SPIE **2280,** 181 (1994).
6. D. L. Voronov, R. Cambiea, R. M. Feshchenkoc, E. M. Gulliksona, H. A. Padmorea, A. V. Vinogradovc, and V. V. Yashchuk, Proc. SPIE **6705,** 67050E (2007).
7. L. Solymar and D. J. Cooke, *Volume Holography and Volume Gratings* (Academic Press, New York, 1981).
8. A. V. Vinogradov, Proc. SPIE **2515,** 22 (1995).
9. H. C. Kang, G. B. Stephenson, C. Liu, R. Conley, A. T. Macrander, J. Maser, S. Bajt, and H. N. Chapman, Appl. Phys. Lett. **86,** 151109 (2005).
10. E. A. Bugaev, R. M. Feshchenko, A. V. Vinogradov, D. L. Voronov, V. A. Tokarev, and V. P. Petukhov, Proc. SPIE **5918,** 591817 (2005).
11. J. Maser and G. Schmahl, Opt. Commun. **89,** 355 (1992).
12. V. E. Levashov and A. V. Vinogradov, Appl. Opt. **32,** 1130 (1993).
13. G. Schneider, Appl. Phys. Lett. **71,** 2242 (1997).
14. Q. Huang, H. Li, J. Zhu, T. Sang, Z. Wang, and L. Chen, Acta Photon. Sin. (in Chinese) **38,** 2299 (2009).
15. Q. Huang, H. Li, J. Zhu, X. Wang, L. Jiang, Z. Wang, and Y. Tang, High Power Laser Part. Beams (in Chinese) **23,** 1659 (2011).
16. C. Liu, R. Conley, and A. T. Macrander, Proc. SPIE **6317,** 63170J (2006).
17. Y. Wang, H. Zhou, L. Zhou, R. L. Headrick, A. T. Macrander, and A. S. Özcan, J. Appl. Phys. **101,** 023503 (2007).
18. M. Tan, H. Li, Q. Huang, H. Zhou, T. Huo, X. Wang, and J. Zhu, Chin. Opt. Lett. **9,** 023102 (2011).
19. Q. Huang, J. Zhu, H. Li, Z. Shen, X. Wang, Z. Wang, and Y. Tang, Chin. Opt. Lett. **10,** 013103 (2012).
20. V. Holý, U. Pietsch, and T. Baumbach, *High-resolution X-ray Scattering from Thin Films and Multilayers* (Springer, Berlin, 1999).